Identification of Organic Nitrates in the NO₃ Radical Initiated Oxidation of α-Pinene by Atmospheric Pressure Chemical Ionization Mass Spectrometry

Véronique Perraud, Emily A. Bruns, Michael J. Ezell, Stanley N. Johnson, John Greaves, and

Barbara J. Finlayson-Pitts*

Department of Chemistry, University of California Irvine, Irvine, CA 92697-2025

July 01, 2010

*Author to whom correspondence should be addressed: phone (949) 824-7670; fax (949) 824-2420; e-mail bjfinlay@uci.edu

Summary

Number of pages: 20
2 Figures
3 Tables
3 Schemes

Additional Experimental Details.

Atmospheric pressure chemical ionization triple quadrupole mass spectrometry: In APCI-MS, positive ion formation occurs via a corona discharge that generates protonated water clusters from trace water present in the system. For analytes with higher proton affinities (PA) than the water clusters, transfer of a proton forms an $[M + H]^+$ ion which generally can be detected and measured, although some fragmentation of this parent ion can occur. The APCI-MS instrument was operated in two different modes in addition to the Q1 single quadrupole scan. In the product ion scan mode (designated MS/MS throughout), ions of chosen m/z exit the first quadrupole (Q1) and are collisionally dissociated using nitrogen gas. The resulting fragment ions are scanned in the last quadrupole (Q3), producing a mass spectrum that shows characteristic fragmentation patterns for the ion selected in Q1; this is useful for elucidating the structure of the chosen ion. In the precursor ion scan mode (PIS), Q3 is fixed at a particular m/z and Q1 is scanned to determine precursors to the Q3 selected ion. Thus, the PIS mode is useful for establishing whether a given ion observed in the Q1 scan is a parent $[M + H]^+$ ion or a fragment from a larger ion.

Reagents: The nitrate radical was generated via the thermal decomposition of N_2O_5:

$$N_2O_5 \leftrightarrow NO_2 + NO_3$$

N_2O_5 was prepared in a glass vacuum rack by reacting a 2.4% O_3/O_2 mixture from a discharge ozone generator with NO_2, and was stored in a dry ice-acetone bath (-78 °C) until needed (no longer than six days to minimize surface loss of the N_2O_5 by its conversion to nitric acid). The cold trap containing the N_2O_5 was warmed to vaporize a portion of the sample into a calibrated, previously evacuated and conditioned, 0.410 L bulb until the desired pressure was reached. Nitrogen was then added to give a total pressure of 1 atm.

Before each experiment, α-pinene [(1R)-(+)-α-pinene, Sigma Aldrich, > 99%] was purified by passage through a glass column of neutral aluminium oxide (chromatography grade, J.T. Baker Chemical Company) to remove oxidized impurities. After this treatment, GC-MS analysis showed only a β-pinene impurity (1.6%). The standard, *cis*-pinonic acid (Aldrich, 98%), was used as received.

Gas-phase measurement of α-pinene: Measurements of α-pinene in the reaction chamber were made by collecting a gas sample in a 1 mL stainless steel loop followed by analysis by GC-MS (Agilent 7890A GC and a 5975C inert XL EI/CI MSD with triple-axis detector) with a Supelco SLB^{TM}-5ms column of 20 m length, 0.18 mm internal diameter, and a 0.18 μm film thickness using single ion monitoring on *m/z* 91. The use of a NIST traceable standard of 560 ppb α-pinene diluted in nitrogen (Scott-Marin) was used for calibration. Helium (Ultra High Purity, Oxygen Services Company) was used as the carrier gas. The oven temperature gradient started at 0 °C obtained by cooling using vapor from a liquid nitrogen tank (hold 1 min) and increased at 40 °C min^{-1} to 240 °C. The experimentally determined limit of detection for α-pinene was 1 ppb.

Denuder efficiency experiments: Independent tests were carried out to measure the efficiency of the carbon denuder for removal of gases as well as the transmission efficiency for particles. Prior to all measurements, the denuders were reconditioned overnight under a stream of nitrogen (Ultra High Purity, Oxygen Services Company) at ~ 75 °C. The denuder removed more than 99% of the gases in experiments using 200 ppb α-pinene and 200 ppb acetone (HPLC grade, EMD Chemicals). Given the large signals from the gas phase compared to the particles (Figure 1 in text), a small contribution from the gas phase to the MS assigned to particles in Figure 1b cannot be ruled out with certainty. Transmission of particles

formed during the ozonolysis of α-pinene through the denuder was experimentally measured

to be greater than 92% at a flow of 1.0 L min^{-1} and there was no change in the particle size

distribution as measured by particle size spectrometers described below. The removal of

N_2O_5/NO_3 was also tested by sampling a mixture formed by reacting 1 ppm O_3 with 4 ppm

NO_2 in an aerosol flow tube (*SI*) into a long path-length (64 m) FTIR apparatus either directly

or after passing through the denuder. No N_2O_5 could be detected after passing through the

denuder, indicating greater than 95% removal.

Size distribution of particles: The size distribution of the particles was measured using a

scanning mobility particle sizer (SMPS) consisting of a long differential mobility analyzer

(DMA, TSI Model 3080) and a condensation particle counter (CPC, TSI Model 3022A), and

an aerodynamic particle sizer (APS, TSI Model 3321).

Filter sampling of particles: Particles generated in a 300 L Teflon® chamber experiment

using 2 ppm of α-pinene and 1 ppm of N_2O_5 were collected, after passage through the

denuder, on quartz-fiber filters (Tissuquartz™, 37 mm diameter) mounted in a 3-piece

polypropylene SureSeal air monitoring cassette (SKC). Prior to use, the filters were baked in

air at ~ 475 °C overnight to remove organic contaminants. A total air sample volume of ~

270-290 L was passed through the filters.

Filter analysis: After sampling, filters were extracted using 2 mL of acetonitrile (HPLC

grade, EMD Chemicals) with sonication for 10 minutes. The extracts were analyzed using

electrospray ionization mass spectrometry [ESI-ToF-MS (negative ion detection)] and

GC/MS. ESI-ToF-MS was conducted using a LCT Premier mass spectrometer (Waters)

operating in the negative ionization mode (mass range: 100 to 2000 Da). Samples were

introduced via a 6-port injection valve directly into the solvent stream using flow injection analysis (FIA). The sample injection volume was 10 µL and the mobile phase was methanol (Optima®LC-MS grade, Fischer Scientific) with a flow rate of 0.1 mL min^{-1}. The temperature of the source was 150 °C. A 500 L hr^{-1} flow of nitrogen maintained at 150 °C was used as the desolvation gas. Electrospray and sample cone voltages were 3000 V and 30 V respectively. Data were acquired using MassLynx^{TM} Software (Waters).

GC-MS analysis was conducted on an Agilent Model 6850 Series II GC coupled to a Model 5975B VL mass selective detector (MSD). Separation was performed on a DB-5ms column of 60-m length, 0.25-mm internal diameter, and 0.25-µm film thickness (Agilent). A portion of the quartz-fiber filter extracts (200 µL) was evaporated into dryness under a gentle stream of nitrogen, redissolved in 20 µl of dichloromethane (OmniSolv, EMD chemicals), and 3 µL of the redissolved extract was then injected onto the GC-MS (splitless mode). The column was temperature programmed as follows: 60 ºC (hold 5 min) followed by a temperature ramp at 3 ºC min^{-1} to reach 240 ºC (hold for 5 min). The inlet temperature was 160 °C and the carrier gas was helium (Ultra High Purity, Oxygen Services Company) with a flow rate of 1.0 mL min^{-1}. Temperatures of the transfer line, source and quadrupole were 275 °C, 230 °C and 150 °C respectively. Electron ionization (70 eV) and scanning *m/z* from 35 to 550 allowed the identification of compounds by comparison of their mass spectra with the NIST library (identification match > 90%) or with spectra obtained from authentic standards.

Prior to analysis, carboxylic acids and alcohols from the quartz fiber filter extracts were derivatized using N,O-bis(trimethylsilyl)trifluoroacetamide (BSTFA) reagent with trimethylchlorosilane catalyst (Supelco, BSTFA + TMC, 99:1) in pyridine (99% GR ACS, EMD Chemicals) (*S2*). The inlet temperature was heated to 280 °C and the trimethylsilyl

derivatives were separated using a different column temperature program: starting at 84 °C (hold 1 min), increasing at 10 °C min^{-1} to 200 °C (hold 6 min), followed by a second ramp at 10 °C min^{-1} to 280 °C. The final temperature was held for 15 min.

Accurate mass measurement: Atmospheric pressure chemical ionization time-of-flight mass spectrometry (APCI-ToF-MS) was conducted on a LCT Premier mass spectrometer (Waters) using the positive ionization mode (mass range: 100 to 300 Da). Samples were introduced via a 6-port injection valve directly into the solvent stream for FIA. The sample injection volume was 10 µL and the mobile phase was methanol (Optima$^®$ LC-MS grade, Fischer Scientific) with a flow rate of 0.1 mL min^{-1}. The APCI probe and the source were maintained at 500 °C and 100 °C respectively. The corona discharge current was 5 µA and the sample cone voltage was 30 V. Addition of a small amount of a dilute caffeine solution (194.1908 Da) provided the reference lock mass for exact mass measurement to obtain empirical formulae. The analyzer was operated in W mode at a resolution > 8000 FWHM. Data were acquired using MassLynx^{TM} Software (Waters).

Mechanisms of Formation of Products.

Scheme S1 summarizes a simplified mechanism for the formation of the four major products (*S3-8*). Minor products include α-campholene aldehyde, norpinonaldehyde, and α-pinene oxide (*S3, S5-8*). Our experiments were carried out in absence of NO, and the self- and cross reaction of the peroxy radicals is expected to govern the formation of alkoxy radicals, leading to the formation of pinonaldehyde and the hydroxy- and keto-pinane nitrate products. Formation of pinonaldehyde-PAN has been reported to be the major product from the further reaction of pinonaldehyde with NO$_3$ radicals (*S7, S9*).
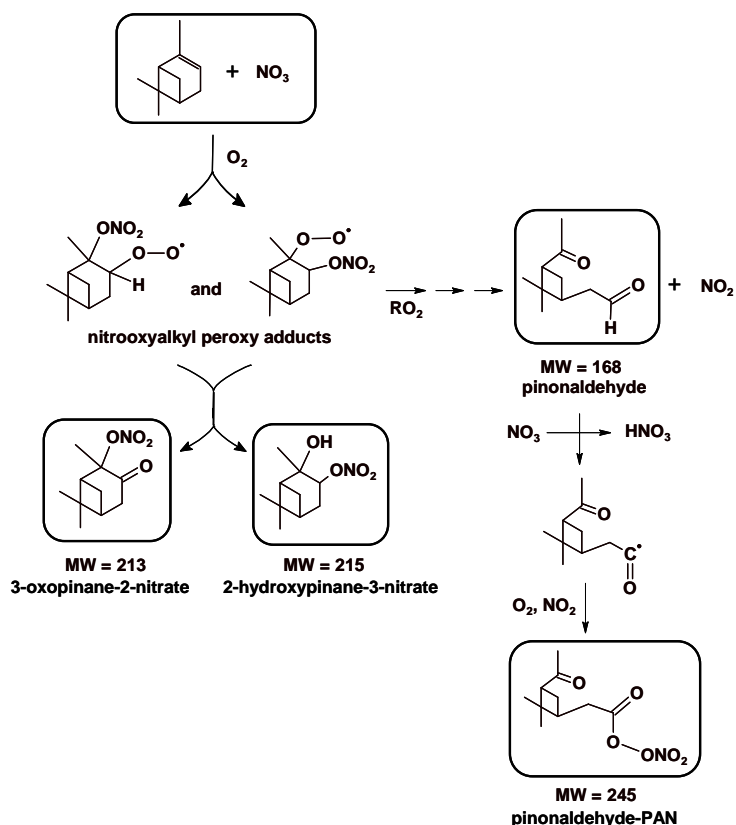
Scheme S1. Partial mechanism for the NO$_3$ radical oxidation of α-pinene to form the major reaction products (see references (*S3, S6, S7*)).

Possible pathways leading to the formation of carbonyl hydroxynitrate products with molecular mass 229 are presented in Scheme S2. Following a similar mechanism to that reported for OH chemistry (*S10-13*), we propose isomerization of the nitrooxyalkoxy radical formed from the addition of NO$_3$ to the double bond of α-pinene via a six-membered transition state. The result is a multifunctional organic nitrate that contains both a carbonyl and an alcohol group. Loss of H$_2$O is expected in the APCI-MS, leading to the formation of a [M + H - H$_2$O]$^+$ fragment ion at *m/z* 212, and this fragment was observed in the Q1 scan of a N$_2$O$_5$/α-pinene chamber experiment presented in Figure 1 in the text.
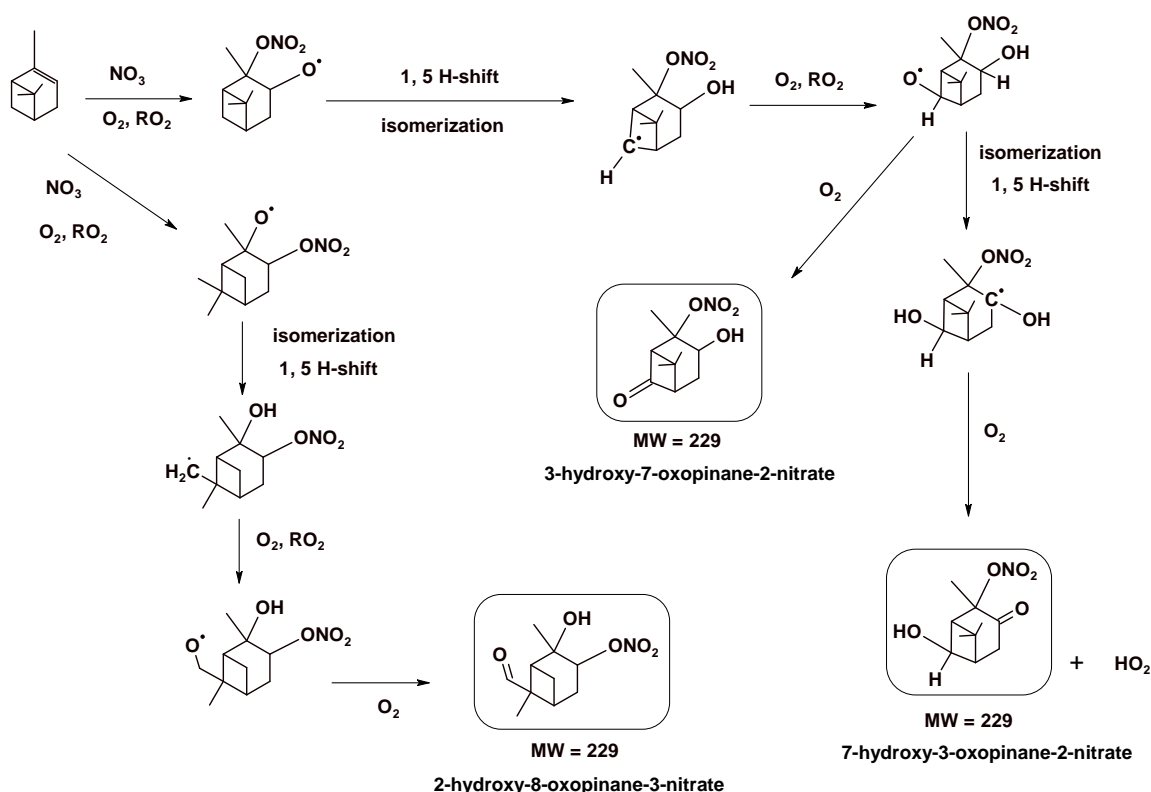
Scheme S2. Potential mechanism for the formation of carbonyl hydroxynitrates responsible for the *m/z* 212 observed in the Q1 scan (Figure 1 in text).

Scheme S3 presents a simplified mechanism for the reaction of pinonaldehyde, a first generation product, with NO_3. Pinonaldehyde reacts with NO_3 with a rate constant $k^{298K} = 2.0 \times 10^{-14}$ molecules cm^{-3} (*S14-17*). While the reaction of pinonaldehyde with NO_3 is ~ 300 times slower than the α-pinene/NO_3 reaction ($k^{298K} = 6.2 \times 10^{-12}$ molecules cm^{-3} (*S17*)), pinonaldehyde continues to react after all the α-pinene has been consumed. Pinonaldehyde-PAN has been reported to be the major reaction product (*S7, 9*). Norpinonaldehyde has been reported as a decomposition product of pinonaldehyde in the OH reaction (S*18, 19*), and a minor product in the α-pinene/NO_3 system (*S5*). The reactivity of norpinonaldehyde towards NO_3 is expected to be similar to that for pinonaldehyde, leading to norpinonaldehyde-PAN. As shown in this study and as reported by Noziere and Barnes (S*9*), abstraction of the tertiary hydrogen by NO_3 constitutes one pathway for the degradation of pinonaldehyde and the formation of (3-acetyl-2,2-dimethyl-3-nitrooxycyclobutyl)acetaldehyde (MW 229). The latter

S9

is expected to be a minor product since the contribution of the tertiary hydrogen abstraction is

small and the alkoxy radical precursor can also decompose and undergo isomerization via

internal hydrogen shifts (*S20*). A large increase in the MS signals assigned to pinonaldehyde-

PAN, norpinonaldehyde, norpinonaldehyde-PAN, and (3-acetyl-2,2-dimethyl-3-

nitrooxycyclobutyl)acetaldehyde (MW 229) and decrease in pinonaldehyde as a function of

reaction time is consistent with these products being secondary products formed from

pinonaldehyde secondary chemistry.
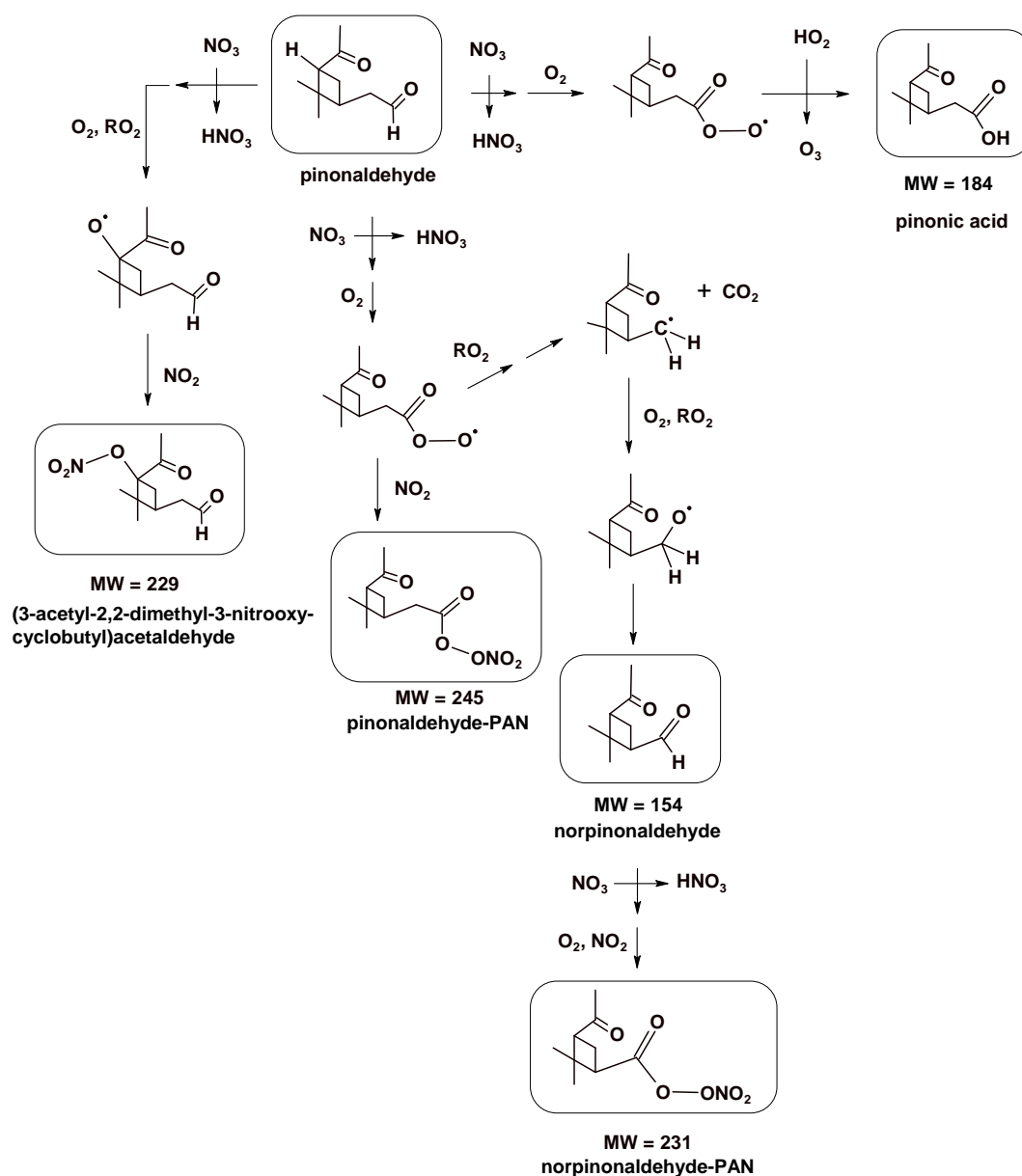
Scheme S3. Partial mechanism for the oxidation of pinonaldehyde by NO_3 to give the five observed products shown.

The relative amounts of the products formed from this chemistry in the atmosphere will be somewhat different than measured in the present studies where relatively high concentrations of NO_2 are present from the N_2O_5 decomposition, but NO concentrations are small. For example, the formation of the PAN products is emphasized at higher NO_2 concentrations.

Pinonic Acid Analysis.

Figure S1 shows MS/MS scans of the $[M + H]^+$ ion at *m/z* 185 from a N_2O_5/α-pinene experiment (4 ppm N_2O_5, 1.4 ppm α-pinene, 110 min reaction time) and from a commercial sample of *cis*-pinonic acid. The two scans show an identical fragmentation pattern, including a loss of water from the $[M + H]^+$ peak leading to an intense fragment at *m/z* 167, as well as a number of smaller fragments corresponding to loss of H_2O, CO and C_2H_2O. These MS/MS scans are also in agreement with previously reported MS fragmentation for pinonic acid (*S21*). The good agreement between Figure S1a and S1b, as well as the detection of pinonic acid in the GC-MS and ESI-ToF-MS (negative ion detection) analysis of filter extracts from N_2O_5/α-pinene experiments (data not shown) confirms the identification of *m/z* 185 as the parent $[M + H]^+$ ion for pinonic acid observed in the N_2O_5/α-pinene experiment.

Following a similar mechanism to that reported for OH/α-pinene chemistry (*S21-23*), we propose that the formation of pinonic acid occurs by abstraction of the aldehydic hydrogen of pinonaldehyde, followed by reaction with HO_2 (Scheme S3). This HO_2 reaction with pinonaldehyde has also been reported to be a source of peroxy pinonic acid (*S18, 22*), which would give an $[M + H]^+$ peak at *m/z* 201. However, the *m/z* 201 cannot be assigned unequivocally to peroxy pinonic acid formed in the reaction of NO_3 with pinonaldehyde. For example, Hansel and Wishthaler (*S24*) observed in the PTR-MS spectrum of PAN, a fragment

corresponding to a peroxy carboxylic acid, which they proposed was formed from secondary reactions of the protonated PAN:

$$RC(O)OONO_2H^+ + H_2O \rightarrow RC(O)OOH_2^+ + HNO_3$$
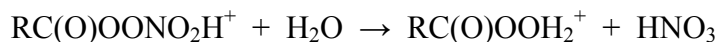
It is therefore possible that pinonaldehyde-PAN undergoes similar chemistry in the source region to give an $[M + H + H_2O - HNO_3]^+$ fragment at m/z 201.
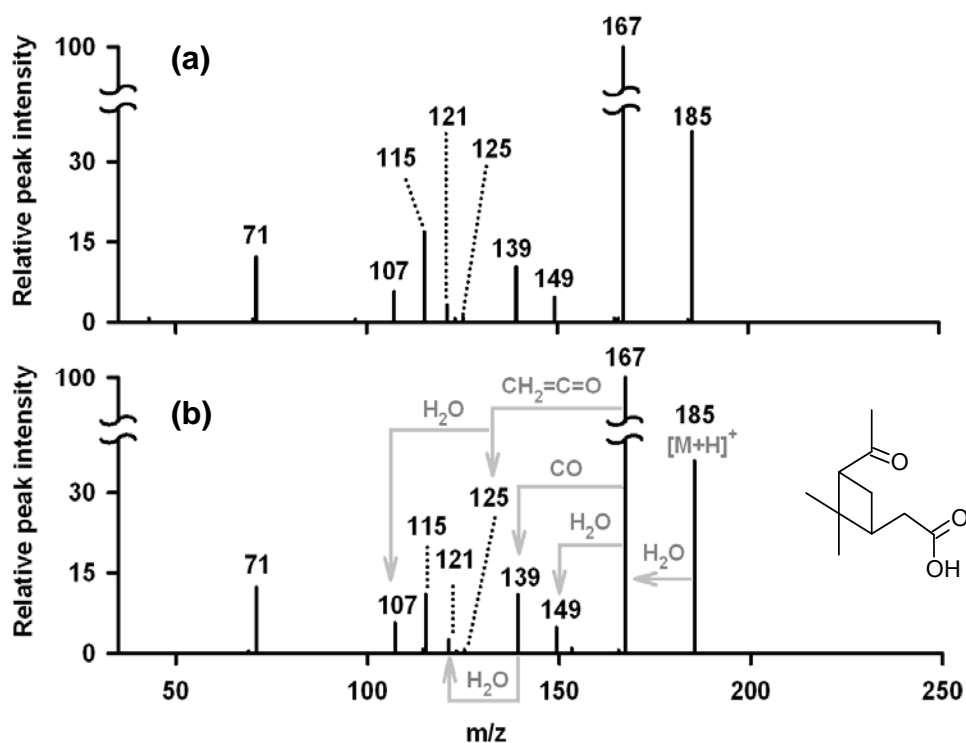

Figure S1. Product ion spectra of m/z 185 from (a) a N_2O_5/α-pinene chamber experiment (4 ppm N_2O_5, 1.4 ppm α-pinene, 110 min reaction time), and (b) the headspace of cis-pinonic acid standard. Both spectra were taken at a collision energy (CE) of 10 eV.

The present studies were carried out with relatively high NO_2 and low NO concentrations (due to the use of the thermal decomposition of N_2O_5 as the NO_3 source), which will favor PAN formation. Under atmospheric conditions where NO_3 is formed and NO is low, the alkyl

peroxy radicals formed in the α-pinene oxidation undergo cross reactions with other RO_2 and HO_2 (*S20*). In the latter case, the formation of hydroperoxides is expected. In air, cross-reaction of RO_2 from the α-pinene reaction with those from other organics is more likely than self-reaction, but generation of the alkoxy radical will then lead for the most part to the same products observed in the present studies. In short, the products identified here are expected to be formed in forested regions.

Details of Precursor and Product Ion (MS/MS) Scans.

Table S1 summarizes the precursor and product ions of the even-numbered mass peaks observed in the Q1 scan in Figure 1 of the text.

Table S1. Precursor and product ions of the even-numbered peaks observed in the Q1 scan of a N_2O_5/α-pinene experiments (4 ppm N_2O_5, 1.4 ppm α-pinene).

Observed m/z peak in Q_1 spectra	Precursor ions (PIS mode)[a]	Product ions (MS/MS mode)[a]	Parent peak identification observed in Q1 scan
198	198 (100%) 200 (1%) 216 (2%) 246 (5%)[b]	198 (100%) 151, - HNO_2 (4%)	fragment ion of 2-hydroxypinane-3-nitrate (MW 215)
200	200 (33%) 246 (100%)	200 (100%) 183, - OH (17%) 198, - H_2 (0.5%) 167, - HO_2 (0.5%) 165, - (OH + H_2O) (6%)	fragment ion of pinonaldehyde-PAN (MW 245)
212	212 (100%)	212 (100%) 166, - NO_2 (6%) 148, - (H_2O + NO_2) (2%)	fragment ion of a carbonyl hydroxynitrate product (MW 229)[c]
214	214 (100%)	214 (100%) 168, - NO_2 (20%) 151, - HNO_3 (41%)	[M + H]+ ion of 3-oxopinane-2-nitrate (MW 213)
216	216 (100%)	216 (100%) 198, - H_2O (9%) 170, - NO_2 (2%) 152, - (H_2O + NO_2) (25%)	[M + H]+ ion of 2-hydroxypinane3-nitrate (MW 215)
228	228 (100%) 246 (44%)	228 (100%) 182, - NO_2 (9%) 163, - (HNO_2 + H_2O) (11%)	fragment ion of pinonaldehyde-PAN (MW 245)
230	230 (100%)	230 (59%) 212, - H_2O (1%) 184, - NO_2 (100%) 166, - (H_2O + NO_2) (3%)	[M + H]+ ion of (3-acetyl-2,2-dimethyl-3-nitrooxycyclobutyl)acetaldehyde (MW 229)
232	232 (100%)	232 (100%) 214, - H_2O (1%) 199, - HO_2 (1%) 186, - NO_2 (3%) 153, - $HOONO_2$ (20%)	[M + H]+ ion of norpinonaldehyde-PAN (MW 229)
246	246 (100%)	246 (100%) 228, - H_2O (0.9%) 200, - NO_2 (92%) 198, - (H_2 + NO_2) (0.6%) 183, - HNO_3 (4%) 167, - $HOONO_2$ (10%)	[M + H]+ ion of pinonaldehyde-PAN (MW 245)

[a]Relative intensities in parentheses correspond to the intensity of each peak ratioed to the base peak (100%); precursor ions and MS/MS scans were recorded at a low collision energy (CE = 5 eV).
[b]Note that the MS/MS of m/z 246 has only a very weak peak at m/z 198, suggesting that pinonaldehyde-PAN does not contribute significantly to m/z 198. The alcohol at m/z 216 is expected to lose water and to be a major source of this peak.
[c]The absence of m/z 230 in the precursor ion scan suggests complete fragmentation of the [M + H]+ peak via loss of water.

Identification of Products in Particles Collected on Filters Using Accurate Mass Measurement.

APCI-ToF-MS in the positive ion mode of filter extracts was used to confirm the identification of some of the peaks observed in the APCI-MS data. Figure S2 shows a typical spectrum. Peaks in common with the Q1 scan from the APCI-MS measurement using the denuder (Figure 1b in text) include *m/z* 151, 167, 169, 185, 198, and 214.

Exact masses were obtained using caffeine (194.0804 Da) as the reference. All assignments were based on the fact that the discrepancy between the measured mass and the calculated masses for the possible elemental compositions was small for the assigned elemental composition and much larger for the next available possibilities (see Table S2). Exact mass measurements established that the peak at *m/z* 169.1229 is due to $C_{10}H_{17}O_2$ and that at *m/z* 151.1123 is due to $C_{10}H_{15}O$, consistent with the $[M + H]^+$ and $[M + H - H_2O]^+$ fragments from pinonaldehyde. The exact difference of 18.0106 Da corresponds to the loss of H_2O. Similarly, this analysis provided elemental compositions of $C_{10}H_{17}O_3$ (exact mass *m/z* 185.1178) and $C_{10}H_{15}O_2$ (exact mass *m/z* 167.1072), consistent with pinonic acid peaks at $[M + H]^+$ and $[M + H - H_2O]^+$. The presence of one additional oxygen compared to pinonaldehyde (exact mass difference = 15.9949 Da) and the exact difference of 18.0106 Da for the two fragments are again consistent with pinonic acid.

The exact mass of *m/z* 214.1079 is an elemental composition of $C_{10}H_{16}NO_4$, corresponding to 3-oxopinane-2-nitrate. Similarly, the exact mass of *m/z* 198.1130, $C_{10}H_{16}NO_3$, corresponds to loss of water from 2-hydroxypinane-3-nitrate, which readily occurs in alcohols, and is likely enhanced by the high temperature of the source so that no parent $[M + H]^+$ appears.

There is a large peak with exact mass at *m/z* 168.1150, corresponding to an elemental composition of $C_{10}H_{16}O_2$ (difference - 8.5 ppm). An alternative elemental composition, $C_6H_{16}O_5$ does not agree well with the measured mass (difference > 82.2 ppm). The exact difference of 45.9929 Da between *m/z* 214.1079 and *m/z* 168.1150 suggests loss of NO_2 from a protonated ion fragment at *m/z* 214.1079, consistent with protonated 3-oxopinane-2-nitrate as the precursor ion to *m/z* 168.1150. The presence of the *m/z* 168 fragment in the APCI-ToF-MS scan but not in the APCI-triple quadrupole-MS measurement can be explained by decomposition of the product at the high temperature of the APCI-ToF-MS source (500 °C) since organic nitrates are well known to decompose thermally to $RO + NO_2$ at high temperatures (> 300 °C) (*S9, S25-28*).
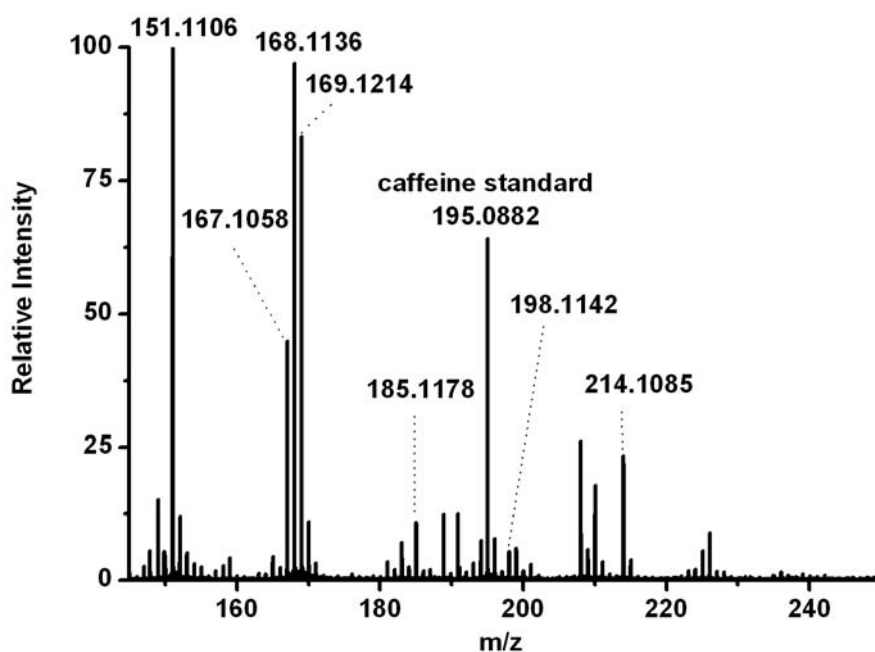
Figure S2. Typical APCI-ToF-MS (positive ion detection) spectrum of a filter extract from a chamber experiment using 1 ppm of N_2O_5 and 2 ppm of α-pinene.

Table S2. Exact mass measurements from APCI-ToF-MS analysis (positive ion detection) on filter extracts from a chamber experiment using 1 ppm of N_2O_5 and 2 ppm of α-pinene.

Observed Mass (*m/z*)	Calculated mass (Da)	Difference (mDa)	Difference (ppm)	Formula
151.1106	151.1123	-1.7	-11.2	$C_{10}H_{15}O$
	151.0970	13.6	89.8	$C_6H_{15}O_4$
	151.1334	-22.8	-151.0	$C_7H_{19}O_3$
167.1058	167.1072	-1.4	-8.4	$C_{10}H_{15}O_2$
	167.0919	13.9	82.9	$C_6H_{15}O_5$
	167.0861	19.7	118.0	$C_{13}H_{11}$
168.1136	168.1150	-1.4	-8.5	$C_{10}H_{16}O_2$
	168.0998	13.8	82.2	$C_6H_{16}O_5$
	168.0939	19.7	117.2	$C_{13}H_{12}$
169.1214	169.1229	-1.5	-8.6	$C_{10}H_{17}O_2$
	169.1076	13.8	81.6	$C_6H_{17}O_5$
	169.1017	19.7	116.3	$C_{13}H_{13}$
185.1178	185.1178	0.0	0.2	$C_{10}H_{17}O_3$
	185.1330	-5.2	-82.2	$C_{14}H_{17}$
	185.1025	15.3	82.6	$C_6H_{17}O_6$
198.1142	198.1130	1.2	6.0	$C_{10}H_{16}NO_3$
	198.1283	-14.1	-71.0	$C_{14}H_{16}N$
	198.0979	16.4	83.0	$C_6H_{16}NO_6$
214.1085	214.1079	0.6	2.6	$C_{10}H_{16}NO_4$
	214.1232	-14.7	-68.6	$C_{14}H_{16}NO$
	214.0927	15.8	73.9	$C_6H_{16}NO_7$

Gas-Particle Partitioning.

Products observed in this study have been detected in the gas phase as well as in the particles. According to Pankow and co-workers (*S29, S30*), the equilibrium partitioning of component *i* between the gas-phase and the particles can be described by a partitioning coefficient $K_{p,i}$ as:

$$K_p = \frac{F_i / TSP}{A_i} = \frac{760 \cdot R.T. f_{om}}{MW_{om} \cdot 10^6 \cdot \varsigma_i \cdot \rho^0_{L,i}} \qquad \text{(S_I)}$$

where F_i (ng m^{-3}) is the concentration of compound *i* in the particles, *TSP* is the total suspended particle concentration in µg m^{-3} and A_i (ng m^{-3}) is the gas phase concentration of compound *i* (*S29, S30*). The ideal gas constant, *R*, is 8.206×10^{-5} m^3 atm mol^{-1} K^{-1}, MW_{om} is the average molecular weight of the given organic matter (*om*), f_{om} is the weight fraction of

the suspended particulate material that constitutes the absorbing *om* phase, ς_i is the activity

coefficient of compound *i* in the particulate phase (generally assumed to be close to unity) and

$p^o_{L,i}$ *is* the saturation vapor pressure of compound *i* at temperature *T* (*S29, S30*). The value of

K_p depends inversely on the saturation vapor pressure ($p^o_{L,i}$) which has not been reported for

many of the products reported here, particularly the organic nitrates. However, a group

contribution method developed by Pankow and Ascher (*S31*) can be used to estimate these

values:

$$\log_{10} p^o_{L,i}(T) = b_0(T) + \sum_k v_{k,i} b_k(T) \qquad\qquad (S_{II})$$

In equation (S_{II}), $v_{k,i}$ is the number of groups of type *k* (*e.g.* carbonyl, nitrate, carboxylic acid)

assigned by Pankow and Ascher (*S31*), $b_k(T)$ is the temperature-dependent contribution term

by each group of type *k*, while $b_o(T)$ is a *T*-dependent constant. Equation (S_{II}) was used to

estimate the vapor pressures that are reported in Table S3.

(S8)   Calogirou, A.; Larsen, B. R.; Kotzias, D., Gas-phase terpene oxidation products: A review. *Atmos. Environ.* **1999,** *33*, 1423-1439.

(S9)   Noziere, B.; Barnes, I., Evidence for formation of a PAN analogue of pinonic structure and investigation of its thermal stability. *J. Geophys. Res.* **1998,** *103*, 25587-25597.

(S10) Orlando, J. J.; Noziere, B.; Tyndall, G. S.; Orzechowska, G. E.; Paulson, S. E.; Rudich, Y., Product studies of the OH- and ozone-initiated oxidation of some monoterpenes. *J. Geophys. Res.* **2000,** *105*, 11561-11572.

(S11) Aschmann, S. M.; Reissell, A.; Atkinson, R.; Arey, J., Products of the gas phase reactions of the OH radical with α- and β-pinene in the presence of NO. *J. Geophys. Res.* **1998,** *103*, 25553-25561.

(S12) Davis, M. E.; Stevens, P. S., Measurements of the kinetics of the OH-initiated oxidation of α-pinene: Radical propagation in the OH plus α-pinene + O_2 + NO reaction system. *Atmos. Environ.* **2005,** *39*, 1765-1774.

(S13) Dibble, T. S., Reactions of the alkoxy radicals formed following OH-addition to α-pinene and β-pinene. C-C bond scission reactions. *J Am. Chem. Soc.* **2001,** *123*, 4228-4234.

(S14) Glasius, M.; Calogirou, A.; Jensen, N. R.; Hjorth, J.; Nielsen, C. J., Kinetic study of gas-phase reactions of pinonaldehyde and structurally related compounds. *Int. J. Chem. Kinet.* **1997,** *29*, 527-533.

(S15) Alvarado, A.; Arey, J.; Atkinson, R., Kinetics of the gas-phase reactions of OH and NO_3 radicals and O_3 with the monoterpene reaction products pinonaldehyde, caronaldehyde, and sabinaketone. *J. Atmos. Chem.* **1998,** *31*, 281-297.

(S16) Hallquist, M.; Wangberg, I.; Ljungstrom, E., Atmospheric fate of carbonyl oxidation products originating from α-pinene and Δ-(3)-carene: Determination of rate of reaction with OH and NO_3 radicals, UV absorption cross sections, and vapor pressures. *Environ. Sci. Technol.* **1997,** *31*, 3166-3172.

(S17) Atkinson, R.; Baulch, D. L.; Cox, R. A.; Crowley, J. N.; Hampson, R. F.; Hynes, R. G.; Jenkin, M. E.; Rossi, M. J.; Troe, J., Evaluated kinetic and photochemical data for atmospheric chemistry: Volume II - Gas phase reactions of organic species. *Atmos. Chem. Phys.* **2006,** *6*, 3625-4055.

(S18) Jaoui, M.; Kamens, R. M., Gas phase photolysis of pinonaldehyde in the presence of sunlight. *Atmos. Environ.* **2003,** *37*, 1835-1851.

(S19) Noziere, B.; Barnes, I.; Becker, K. H., Product study and mechanisms of the reactions of α-pinene and of pinonaldehyde with OH radicals. *J. Geophys. Res.* **1999,** *104*, 23645-23656.

(S20) Finlayson-Pitts, B. J.; Pitts, J. N., Jr. *Chemistry of the Upper and Lower Atmosphere - Theory, Experiments, and Applications*. Academic Press: San Diego, 2000.

(S21) Larsen, B. R.; Di Bella, D.; Glasius, M.; Winterhalter, R.; Jensen, N. R.; Hjorth, J., Gas-phase OH oxidation of monoterpenes: Gaseous and particulate products. *J. Atmos. Chem.* **2001,** *38*, 231-276.

(S22) Kamens, R. M.; Jaoui, M., Modeling aerosol formation from α-pinene plus NO_x in the presence of natural sunlight using gas-phase kinetics and gas-particle partitioning theory. *Environ. Sci. Technol.* **2001,** *35*, 1394-1405.

(S23) Librando, V.; Tringali, G., Atmospheric fate of OH initiated oxidation of terpenes. Reaction mechanism of alpha-pinene degradation and secondary organic aerosol formation. *J. Environ. Manag.* **2005,** *75*, 275-282.

(S24) Hansel, A.; Wisthaler, A., A method for real-time detection of PAN, PPN and MPAN in ambient air. *Geophys. Res. Lett.* **2000,** *27*, 895-898.

(S25) Gaffney, J. S.; Marley, N. A.; Prestbo, E. W., Peroxyacyl nitrates (PANs): Their physical and chemical properties. In *The Handbook of Environmental Chemistry*, Hutzinger, O., Ed. Springer-Verlag: Berlin, 1989; Vol. 4, pp 1-38.

(S26) Kleindienst, T. E., Recent development in the chemistry and biology of peroxyacetyl nitrate. *Res. Chem. Intermed.* **1994,** *20*, 335-384.

(S27) Roberts, J. M., The atmospheric chemistry of organic nitrates. *Atmos. Environ. Part A-General Topics* **1990,** *24*, 243-287.

(S28) Roberts, J. M., PAN and related compounds. In *Volatile Organic Compounds in the Atmosphere*, Koppmann, R., Ed. Blackwell Publishing: 2007; pp 221-268.

(S29) Pankow, J. F., An absorption-model of gas-particle partitioning of organic-compounds in the atmosphere. *Atmos. Environ.* **1994,** *28*, 185-188.

(S30) Pankow, J. F., An absorption-model of the gas aerosol partitioning involved in the formation of secondary organic aerosol. *Atmos. Environ.* **1994,** *28*, 189-193.

(S31) Pankow, J. F.; Asher, W. E., SIMPOL.1: A simple group contribution method for predicting vapor pressures and enthalpies of vaporization of multifunctional organic compounds. *Atmos. Chem. Phys.* **2008,** *8*, 2773-2796.

(S32) Yu, J. Z.; Cocker, D. R.; Griffin, R. J.; Flagan, R. C.; Seinfeld, J. H., Gas-phase ozone oxidation of monoterpenes: Gaseous and particulate products. *J. Atmos. Chem.* **1999,** *34*, 207-258.